Solar Phys (2013) 283:413–428
DOI 10.1007/s11207-013-0225-8

Effect of Variable Background on an Oscillating Hot Coronal Loop

K.S. Al-Ghafri · R. Erdélyi

Received: 27 January 2012 / Accepted: 7 January 2013 / Published online: 1 February 2013

Abstract We investigate the effect of a variable, *i.e.* time-dependent, background on the standing acoustic (*i.e.* longitudinal) modes generated in a hot coronal loop. A theoretical model of 1D geometry describing the coronal loop is applied. The background temperature is allowed to change as a function of time and undergoes an exponential decay with characteristic cooling times typical for coronal loops. The magnetic field is assumed to be uniform. Thermal conduction is assumed to be the dominant mechanism for damping hot coronal oscillations in the presence of a physically unspecified thermodynamic source that maintains the initial equilibrium. The influence of the rapidly cooling background plasma on the behaviour of standing acoustic (longitudinal) waves is investigated analytically. The temporally evolving dispersion relation and wave amplitude are derived by using the Wenzel–Kramers–Brillouin theory. An analytic solution for the time-dependent amplitude that describes the influence of thermal conduction on the standing longitudinal (acoustic) wave is obtained by exploiting the properties of Sturm–Liouville problems. Next, numerical evaluations further illustrate the behaviour of the standing acoustic waves in a system with a variable, time-dependent background. The results are applied to a number of detected loop oscillations. We find a remarkable agreement between the theoretical predictions and the observations. Despite the emergence of the cooling background plasma in the medium, thermal conduction is found to cause a strong damping for the slow standing magneto–acoustic waves in hot coronal loops in general. In addition to this, the increase in the value of thermal conductivity leads to a strong decay in the amplitude of the longitudinal standing slow MHD waves.

Keywords Magnetohydrodynamics (MHD) · Plasmas · Sun: corona · Waves

K.S. Al-Ghafri (✉) · R. Erdélyi
Solar Physics and Space Plasma Research Centre (SP²RC), University of Sheffield, Hicks Building, Hounsfield Road, Sheffield S3 7RH, UK
e-mail: app08ksa@sheffield.ac.uk

R. Erdélyi
e-mail: robertus@sheffield.ac.uk

1. Introduction

Recent consecutive solar observations by high-resolution imaging space telescopes and spectrometers have shown that the solar atmosphere is dynamic in nature and is composed of numerous magnetic structures, of which coronal loops are of the centre of focus in this article. It has been confirmed that these complex structures of the solar corona can support a wide range of magnetohydrodynamic (MHD) waves, which are natural carriers of energy and may be the key to solve the problem of solar coronal heating (see the recent review by, *e.g.*, Taroyan and Erdélyi, 2009; McLaughlin *et al.*, 2011). In particular, one MHD wave mode present in coronal loops has become the centre of attention: the slow magneto–acoustic mode. The slow (propagating and standing) MHD waves are extensively supported by the solar coronal structures and are observed to be rapidly damped (Wang *et al.*, 2003a, 2003b; De Moortel, 2009; Wang, 2011).

Propagating intensity disturbances were first detected by the *Ultraviolet Coronagraph Spectrometer* onboard the *Solar Heliospheric Observatory* (SOHO/UVCS) along coronal plumes (Ofman *et al.*, 1997, 1999, 2000a), and were identified as slow magneto–acoustic waves (Ofman *et al.*, 1999). Subsequently, similar intensity disturbances were observed in coronal loops by the *Transition Region and Coronal Explorer* (TRACE: Nightingale *et al.*, 1999; Schrijver *et al.*, 1999; De Moortel *et al.*, 2000; McEwan and De Moortel, 2006) and the *EUV Imaging Telescope* onboard the *Solar Heliospheric Observatory* (SOHO/EIT: Berghmans and Clette, 1999). Nakariakov *et al.* (2000) found that the slow MHD wave evolution is affected by dissipation and gravitational stratification. Erdélyi and Taroyan (2008) and Wang *et al.* (2009) have detected longitudinally propagating slow MHD waves with a period of about five minutes in the transition region and five coronal lines at the footpoint of a coronal loop by *Hinode*/EIS. The source of these oscillations is suggested to be the leakage of the *p*-modes from the photosphere region through the chromosphere and transition region into the corona (De Pontieu *et al.*, 2005).

Oscillations interpreted as longitudinal standing (slow) magneto–acoustic waves have been observed in hot ($T > 6$ MK) active-region loops by the *Solar Ultraviolet Measurement of Emitted Radiation* (SUMER) spectrometer onboard SOHO (Wang *et al.*, 2002, 2003b; Taroyan *et al.*, 2007). These oscillations have periods in the range of 8.6 to 32.3 minutes with decay times of $3.1 - 42.3$ minutes and amplitudes between 12 and 353 km s^{-1} (Wang *et al.*, 2005). Moreover, Mariska (2005) has reported Doppler-shift oscillations during solar flares with *Yohkoh* in a high-temperature region reaching $12 - 14$ MK. These oscillations are interpreted in terms of standing slow-mode MHD waves (Mariska, 2006). Evidence for the standing slow mode can be supported by the phase relationship between velocity and intensity where a quarter-period phase difference is a characteristic of standing waves while propagating waves exhibit an in-phase relationship. Therefore, an approximate quarter-period delay of the intensity variations behind the Doppler shift strongly supports that the oscillations observed by SUMER are slow standing modes. The observed oscillations in coronal loops indicate that the standing slow modes are likely triggered by micro-flares, which are produced by impulsive heating (Mendoza-Briceño *et al.*, 2002). In a recent work, Taroyan and Bradshaw (2008) found that longitudinal standing waves can be excited in cooler EUV loops under the effect of all important mechanisms such as gravitational and thermal stratification, losses, *etc*. According to this study, hot loops are not only the origin of the standing waves but these waves can also be formed in cooler loops.

Today, the damping of slow magneto–acoustic waves has become the subject of remarkable observational and theoretical attention because the damping timescale of the waves may be able to disclose the physical processes that dominate the energy of the coronal loop in

which they are detected. The majority of theoretical and numerical studies on damping of propagating and standing slow MHD waves show that the understanding of dominant mechanisms of rapid damping can be captured from a 1D linear (Sigalotti *et al.*, 2007) or nonlinear model (Wang, 2011). For instance, Ofman and Wang (2002) and Mendoza-Briceño *et al.* (2004) found that the standing MHD waves are strongly damped because of thermal conduction in a nonlinear model, whereas the linear MHD model of Sigalotti *et al.* (2007) indicated that the individual influence of thermal conduction or viscosity is not enough to account for the observed damping. In a static 1D isothermal medium, De Moortel and Hood (2003) investigated the behaviour of both propagating and standing slow MHD waves in the presence of thermal conduction and compressive viscosity. The authors found that thermal conduction is the dominant damping mechanism of thermal and magneto–acoustic waves in coronal loops. They claimed that the thermal mode is purely decaying in the case of standing waves, but is oscillatory and decaying in the case of driven waves. Moreover, Morton *et al.* (2010) have shown that radiative cooling causes a damping of the slow mode by up to 60 % within characteristic lifetimes.

Mendoza-Briceño *et al.* (2004) studied the influence of gravitational stratification on damping of standing MHD waves in hot coronal loops and found that enhanced nonlinear viscous dissipation due to gravity may reduce the damping times by about 10 – 20 % compared to the unstratified loops. In contrast to most recent work, Sigalotti *et al.* (2007) found that thermal conduction can only be considered as a damping mechanism when the compressive viscosity is added to the model. Bradshaw and Erdélyi (2008) reported that the radiation due to a non-equilibrium ionisation balance could shorten the wave-damping timescale by up to 10 % compared to the equilibrium case. Verwichte *et al.* (2008) showed that shock dissipation at large amplitudes gives rise to enhancement of the damping rate, which is up to 50 % higher than given by thermal conduction alone. In non-isothermal, hot, gravitationally stratified coronal loops, Erdélyi *et al.* (2008) investigated the damping of standing slow (longitudinal) waves and found that the decay time of waves decreases with the increase of the initial temperature. In addition to this, the authors derived a relation between the damping time and the parameter determining the apex temperature in the form of a second-order scaling polynomial. In all of these earlier studies, the background (equilibrium) plasma was considered to be time-independent. This is certainly a working model as long as the background plasma changes occur on timescales much longer than typical perturbation timescales. In a recent theoretical work by Erdélyi *et al.* (2011), the cooling of the background plasma due to thermal conduction has been found to *decrease* the rate of damping of the propagating magneto–acoustic waves in a weakly stratified atmosphere where temporal changes in the slowly evolving equilibrium were considered. The cooling temperature profile is found by solving the background-plasma equations algebraically where thermal conduction is present in the background equilibrium.

In this study, we examine how the cooling background state affects the longitudinal *standing* waves in a uniform magnetised plasma. The additional complexity of a time-dependent background is another step on the way to modelling hot coronal loops. The cooling of the background plasma is assumed to be dominated by a physically unspecified thermodynamic source where the plasma is assumed to be cooling in time with an exponential profile in accordance with observations. The coefficient of thermal conductivity is presumed to be varying as a function of time to investigate how the variation of thermal conduction influences the behaviour of standing slow-mode waves. The geometry of the coronal loop is described by a semi-circular shape. An analytical solution for the time-dependant amplitude of the standing slow MHD waves is derived using the Wenzel–Kramsers–Brillouin (WKB) theory with the aid of properties of Sturm–Liouville problems. The results show that thermal conduction causes a significant amplitude variation of the standing magneto–acoustic

Figure 1 Coronal loop.

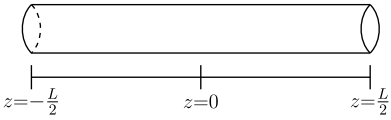

modes with time. The wave amplitudes are found to suffer damping due to the effect of thermal conduction. The influence of the ratio change of the period of standing oscillation to the cooling time scale on the damping rate of hot-loop oscillations seems to be highly efficient, where increasing the value of this ratio rapidly deceases the damping strength.

2. The Model and Governing Equations

Consider a uniformly magnetised plasma in which the temperature is changing as function of time due to a physically unspecified thermodynamic source, and where the density is a constant. The magnetic field in a coronal-loop model of length L is assumed to be uniform and aligned along the z-axes, *i.e.* $\mathbf{B}_0 = B_0\hat{\mathbf{z}}$ (see Figure 1). Therefore, the background state can be described as follows:

$$T_0 = T_0(t), \tag{1}$$

$$p_0 = p_0(t), \tag{2}$$

$$\rho_0 = \text{const}, \tag{3}$$

$$B_0 = \text{const}, \tag{4}$$

$$\epsilon = \frac{P}{\tau_c} \ll 1. \tag{5}$$

Here T_0, p_0, ρ_0, and B_0 are the background quantities identifying the temperature, pressure, density, and magnetic field; P is the period of the loop oscillation, and τ_c is the cooling-time scale.

The governing MHD equations for the background plasma take the form

$$\frac{\partial \rho}{\partial t} + \nabla.(\rho \mathbf{v}) = 0, \tag{6}$$

$$\rho \frac{\partial \mathbf{v}}{\partial t} + \rho(\mathbf{v}.\nabla)\mathbf{v} = -\nabla p + \frac{1}{\mu_0}(\nabla \times \mathbf{B}) \times \mathbf{B}, \tag{7}$$

$$\frac{R}{\tilde{\mu}}\rho^{\gamma}\left[\frac{\partial}{\partial t}\frac{T}{\rho^{\gamma-1}} + (\mathbf{v}.\nabla)\frac{T}{\rho^{\gamma-1}}\right] = (\gamma-1)\nabla(\kappa_{\parallel}\nabla T) + \mathcal{L}, \tag{8}$$

$$p = \frac{R}{\tilde{\mu}}\rho T, \tag{9}$$

$$\frac{\partial \mathbf{B}}{\partial t} = \nabla \times (\mathbf{v} \times \mathbf{B}), \tag{10}$$

where $\mathbf{v}$ is the flow velocity, $\mathbf{B}$ is the magnetic field, g is the gravity, μ_0 is the magnetic permeability of free space, γ is the ratio of specific heats, R is the gas constant, $\tilde{\mu}$ is the mean molecular weight, T is the temperature, $\nabla(\kappa_{\parallel}\nabla T)$ is the thermal conduction term where $\kappa_{\parallel} = \kappa_0 T^{5/2}$, $\mathcal{L}$ is a physically unspecified thermodynamic source term, and ρ and p are the plasma density and pressure.

Assuming that there is no background flow and the background density is constant, the previous equations determining the background plasma state reduce to

$$v_0 = 0, \quad \rho_0 = \text{const}, \tag{11}$$

$$\nabla p_0 = 0, \tag{12}$$

$$p_0 = \frac{R}{\tilde{\mu}} \rho_0 T_0, \quad i.e.\ p_0 \sim T_0, \tag{13}$$

$$\frac{R}{\tilde{\mu}} \rho_0 \frac{\mathrm{d}T_0}{\mathrm{d}t} = \mathcal{L}, \tag{14}$$

where the 0 index denotes the background quantity. The observed cooling of coronal loops has been shown to be well-approximated by an exponential profile for radiatively cooling loops (Aschwanden and Terradas, 2008; Morton and Erdélyi, 2009, 2010). More recently, Erdélyi *et al.* (2011) found that the temperature decreases exponentially in time due to thermal conduction in hot coronal loops. As a result, we assume here that the cooling temperature profile of coronal loops has the form

$$T_0 = T_{0i} \exp\left(-\frac{t}{\tau_c}\right), \tag{15}$$

where T_{0i} is the initial temperature at $t = 0$.

Let us perturb the background state, where all variables can be written in the form

$$f(z,t) = f_0(t) + f_1(z,t),$$

where the subscript 1 indicates the perturbed quantities. In this study we consider longitudinal motions only, *i.e.* $\mathbf{v} = v\hat{\mathbf{z}}$, so the linearised perturbed MHD equations in a 1D system are

$$\frac{\partial \rho_1}{\partial t} + \rho_0 \frac{\partial v_1}{\partial z} = 0, \tag{16}$$

$$\rho_0 \frac{\partial v_1}{\partial t} = -\frac{\partial p_1}{\partial z}, \tag{17}$$

$$\frac{R}{\tilde{\mu}} \left[\rho_1 \frac{\mathrm{d}T_0}{\mathrm{d}t} + \rho_0 \frac{\partial T_1}{\partial t} + (\gamma - 1)\rho_0 T_0 \frac{\partial v_1}{\partial z} \right] = (\gamma - 1)\kappa_0 T_0^{5/2} \frac{\partial^2 T_1}{\partial z^2}, \tag{18}$$

$$p_1 = \frac{R}{\tilde{\mu}} \{\rho_0 T_1 + T_0 \rho_1\}. \tag{19}$$

Here $v_1 \equiv v_{1z}$ is the longitudinal velocity perturbation. It is clear that there are no terms exhibiting the magnetic field but the standing waves are still guided by the magnetic field. Non-dimensionalisation will be used to simplify the 1D governing Equations (16)–(19). The dimensionless quantities are introduced as

$$\begin{aligned} &\tilde{t} = \frac{t}{P}, \quad \tilde{z} = \frac{z}{L}, \quad c_{si} = \frac{L}{P}, \quad \tilde{p}_0 = \frac{p_0}{p_{0i}}, \quad \tilde{T}_0 = \frac{T_0}{T_{0i}}, \\ &c_{si}^2 = \frac{\gamma p_{0i}}{\rho_0}, \quad \tilde{\rho}_1 = \frac{\rho_1}{\rho_0}, \quad \tilde{p}_1 = \frac{p_1}{p_{0i}}, \quad \tilde{T}_1 = \frac{T_1}{T_{0i}}, \quad \tilde{v}_1 = \frac{v_1}{c_{si}}, \end{aligned} \tag{20}$$

where the subscript i represents the value of the quantity at $t = 0$, L is the loop length, and c_{si} is the initial sound speed.

Now, we aim to find the governing equation for the perturbed velocity, which leads to revealing the behaviour of the standing magneto–acoustic mode subject to initial conditions generated in a hot coronal loop. Using the continuity and ideal gas law equations, Equation (18) in terms of dimensionless variables, removing the tilde for the sake of simplicity, takes the form

$$\frac{\partial^2 v_1}{\partial t^2} - T_0 \frac{\partial^2 v_1}{\partial z^2} = \frac{-\sigma}{\gamma} T_0^{5/2} \frac{\partial^3 T_1}{\partial z^3}, \quad \sigma = \frac{(\gamma - 1)\tilde{\mu}\kappa_0 T_{0i}^{5/2}}{RL\sqrt{\gamma\, p_{0i}\, \rho_0}}, \tag{21}$$

where σ is defined as thermal ratio and is found to be a small quantity under typical coronal conditions (*e.g.* De Moortel and Hood, 2003), demonstrated here as

$$\begin{cases} T_0 = 6 \times 10^5 - 5 \times 10^6 \text{ K}, \\ \rho_0 = 1.67 \times 10^{-12} \text{ kg m}^{-3}, \\ \kappa_{\parallel} = 10^{-11}\, T_0^{5/2} \text{ W m}^{-1} \text{ deg}^{-1}, \\ \tilde{\mu} = 0.6, \\ R = 8.3 \times 10^3 \text{ m}^2 \text{ s}^{-2} \text{ deg}^{-1}, \\ \gamma = 5/3, \\ L = 10^8 \text{ m}, \end{cases} \tag{22}$$

giving characteristic values of $\sigma \in [0.0068, 0.48]$ for $T \in [6 \times 10^5, 5 \times 10^6]$ in K.

Equation (21) with the aid of Equation (19) is

$$\frac{1}{T_0^{7/2}} \left(\frac{\partial^2 v_1}{\partial t^2} - T_0 \frac{\partial^2 v_1}{\partial z^2} \right) = \frac{-\sigma}{\gamma} \frac{\partial^3}{\partial z^3} \left[\frac{p_1}{T_0} - \rho_1 \right]. \tag{23}$$

Differentiating with respect to time and, using Equations (16) and (17), we obtain

$$\frac{\partial}{\partial t} \left[\frac{1}{T_0^{7/2}} \left(\frac{\partial^2 v_1}{\partial t^2} - T_0 \frac{\partial^2 v_1}{\partial z^2} \right) \right] = \frac{\sigma}{\gamma} \left[\frac{\gamma}{T_0} \frac{\partial^4 v_1}{\partial t^2 \partial z^2} + \gamma \frac{\mathrm{d}}{\mathrm{d}t} \left(\frac{1}{T_0} \right) \frac{\partial^3 v_1}{\partial t \partial z^2} - \frac{\partial^4 v_1}{\partial z^4} \right], \tag{24}$$

which is the governing equation and can be recast to a convenient form for subsequent analysis:

$$\begin{aligned} \frac{\partial}{\partial t} \left(\frac{\partial^2 v_1}{\partial t^2} - T_0 \frac{\partial^2 v_1}{\partial z^2} \right) &= \frac{7}{2} \frac{1}{T_0} \frac{\mathrm{d}T_0}{\mathrm{d}t} \left(\frac{\partial^2 v_1}{\partial t^2} - T_0 \frac{\partial^2 v_1}{\partial z^2} \right) \\ &\quad - \sigma T_0^{3/2} \frac{\mathrm{d}T_0}{\mathrm{d}t} \frac{\partial^3 v_1}{\partial t \partial z^2} + \sigma T_0^{5/2} \frac{\partial^2}{\partial z^2} \left(\frac{\partial^2 v_1}{\partial t^2} - \frac{T_0}{\gamma} \frac{\partial^2 v_1}{\partial z^2} \right). \end{aligned} \tag{25}$$

There are three different cases of interest for the present context that one can recover from Equation (25).

Case I In the absence of the thermal conduction [σ] and the physically unspecified thermodynamic source in the energy equation [$\mathcal{L} \propto \mathrm{d}T_0/\mathrm{d}t$] the governing equation reduces

to

$$\frac{\partial^2 v_1}{\partial t^2} - c_s^2 \frac{\partial^2 v_1}{\partial z^2} = 0, \quad c_s = \sqrt{T_0} = \text{const}, \tag{26}$$

which has the solution

$$v_1(z,t) = \alpha \cos(\pi z) \cos(\pi c_s t), \tag{27}$$

under the boundary conditions representing a line-tied flux tube perturbed as a semi-circular initial motion proportional to its fundamental mode

$$v_1\left(\pm\frac{1}{2}, t\right) = 0, \qquad v_1(z,0) = \alpha \cos(\pi z), \qquad \frac{\partial v_1}{\partial t}(z,0) = 0, \tag{28}$$

where α is the initial amplitude of the standing wave at $t = 0$. A more general, *e.g.* broad-band, perturbation would, of course, give the solution in the mathematical form of a Fourier series.

Case II In the case of no thermal conduction, *i.e.* $\sigma = 0$, the effect of cooling of the background plasma on the system will be found by solving

$$\frac{\partial^2 v_1}{\partial t^2} - c_s^2 \frac{\partial^2 v_1}{\partial z^2} = 0, \quad c_s(t) = \sqrt{T_0(t)} \neq \text{const}, \tag{29}$$

which is *formally* exactly Equation (26) but with a variable background temperature: $T_0 = T_0(t)$. In spite of the absence of σ, the coefficient of the bracket in the first term on the right-hand side of Equation (25) is originally derived from the thermal-conduction term as seen in Equation (23). Therefore, this term is not added to Equation (29).

Case III The effect of thermal conduction on the behaviour of the standing acoustic waves in the presence of a physically unspecified thermodynamic source will be investigated by solving Equation (25).

3. Analytical Solutions

Our goal now is to find an analytic solution to the governing Equation (29) first in Case II and than to Equation (25) in Case III. Let us point out that Equations (25) and (29) have derivatives multiplied by small factors σ and ϵ, which enables the use of the WKB theory to obtain an approximate solution, where the WKB estimates give good approximations for the lower factor value used.

Case II Let us first start to solve Equation (29) to establish the behaviour of standing magneto–acoustic waves under the influence of background plasma cooling. Assuming that $t_1 = \epsilon t$, which is defined as a slow timescale, meaning the cooling timescale is (much) longer than the period of the oscillations, Equation (29) will reduce to

$$\frac{\partial^2 v_1}{\partial t_1^2} - \frac{c_s^2}{\epsilon^2} \frac{\partial^2 v_1}{\partial z^2} = 0. \tag{30}$$

In line with applying the WKB estimates, let the perturbed velocity variable have the form

$$v_1(z,t_1) = Q(z,t_1)\exp\left(\frac{\mathrm{i}}{\epsilon}\Theta(t_1)\right). \tag{31}$$

The amplitude $[Q]$ can be expanded in the power series as

$$Q(z,t_1) = Q_0 + \epsilon\, Q_1 + \cdots. \tag{32}$$

Substituting Equations (31) and (32) into Equation (30), and taking terms of the order of ϵ^{-3}, we obtain to leading order

$$\frac{\partial^2 Q_0}{\partial z^2} + \frac{\omega^2}{c_\mathrm{s}^2} Q_0 = 0, \tag{33}$$

where $\omega = \mathrm{d}\Theta/\mathrm{d}t_1$. The boundary condition (28) applicable to the function Q_0 is

$$Q_0 = 0 \quad \text{at } z = \pm\frac{1}{2}. \tag{34}$$

Equations (33) and (34) represent a boundary-value problem that determines the frequency of the standing longitudinal (acoustic) mode in a cooling plasma with a varying temperature as a function of time. The general solution that is physically acceptable to this boundary value problem has the form

$$Q_0(z,t_1) = \sum_{n=0}^{\infty} A_n(t_1)\cos\big((2n+1)\pi z\big), \quad \omega_n = (2n+1)\pi c_\mathrm{s},\ n = 0,1,2,\ldots. \tag{35}$$

Then, collecting terms of the order of ϵ^{-2}, we obtain the equation determining the amplitude

$$\frac{\partial^2 Q_1}{\partial z^2} + \frac{\omega^2}{c_\mathrm{s}^2} Q_1 = \frac{\mathrm{i}}{c_\mathrm{s}^2}\left[\frac{\mathrm{d}\omega}{\mathrm{d}t_1} Q_0 + 2\omega\frac{\partial Q_0}{\partial t_1}\right]. \tag{36}$$

It follows from Equation (28) that Q_1 satisfies the boundary conditions

$$Q_1 = 0 \quad \text{at } z = \pm\frac{1}{2}. \tag{37}$$

The boundary-value problem, Equations (36) and (37), which determines Q_1, is a Sturm–Liouville problem and has a solution only when the right-hand side of Equation (36) satisfies the compatibility condition, which is the condition that it is orthogonal to Q_0 (see, Ruderman, 2011). This condition can be obtained by multiplying Equation (36) by Q_0, integrating with respect to z from $-1/2$ to $1/2$ and using the boundary conditions (37). The compatibility condition is eventually written as

$$\int_{-1/2}^{1/2} \frac{\mathrm{i}}{c_\mathrm{s}^2}\left[\frac{\mathrm{d}\omega}{\mathrm{d}t_1} Q_0^2 + 2\omega Q_0\frac{\partial Q_0}{\partial t_1}\right]\mathrm{d}z = 0, \tag{38}$$

which gives the amplitude of the standing wave in the following form

$$A_n(t_1) = A_n(0)\exp\left(\frac{t_1}{4}\right) = A_n(0)\sqrt{\frac{c_\mathrm{s}(0)}{c_\mathrm{s}(t_1)}}. \tag{39}$$

The value of the constant $A_n(0)$ can be found from Equation (35) at $t_1 = 0$, which is in the form of a Fourier cosine series, using the boundary condition (28). Then, the solution (39), in scaled (*i.e.* physical) variables, takes the form

$$A_n(t) = \alpha \sqrt{\frac{c_s(0)}{c_s(t)}}. \tag{40}$$

This result describes the variation of a time-dependent amplitude of longitudinal standing waves in a dynamically cooling magnetic flux tube. Apparently, Equation (40) indicates that the cooling (or heating) leads to an amplification (decrease) of loop oscillation.

It can be seen from this result that the physical complexity of the cooling background is embodied implicitly in the sound speed, *i.e.* the phase speed of the wave propagation. Although the governing equations in Cases I and II have a similar form mathematically, the difference between them occurs in the variability of the phase speed, where the sound speed is constant in Case I and variable in Case II. In general, many similar cases can be found in different studies. The non-adiabatic sound velocity, for instance, reverts to the sound velocity when non-adiabatic terms are neglected from the model of a cylindrical prominence thread with a steady mass flow supporting non-adiabatic MHD waves (Soler *et al.*, 2008), the fast kink speed is converted to a kink speed once the magnetic field is constant in a study of magnetic and density stratification on transversal coronal-loop oscillations (Verth and Erdélyi, 2008), and the tube speed with variable magnetic field falls back to the tube speed with constant magnetic field if there is no magnetic stratification in the tube generating slow longitudinal MHD waves (Luna-Cardozo *et al.*, 2012).

Case III Next, the behaviour of the standing wave in a system dominated by thermal conduction will be obtained by solving the governing Equation (25). Similarly, the WKB theory will be used to find the solution of Equation (25). Let us now introduce two slow variables $t_1 = \epsilon t$ and $\sigma = \epsilon\tilde{\sigma}$, so Equation (25) becomes

$$\frac{\partial^3 v_1}{\partial t_1^3} + \frac{7}{2}\frac{\partial^2 v_1}{\partial t_1^2} - \frac{c_s^2}{\epsilon^2}\frac{\partial^3 v_1}{\partial t_1 \partial z^2} - \tilde{\sigma} c_s^5 \frac{\partial^3 v_1}{\partial t_1 \partial z^2} - \tilde{\sigma} c_s^5 \frac{\partial^4 v_1}{\partial t_1^2 \partial z^2} - \frac{5}{2}\frac{c_s^2}{\epsilon^2}\frac{\partial^2 v_1}{\partial z^2} + \frac{\tilde{\sigma}}{\epsilon^2}\frac{c_s^7}{\gamma}\frac{\partial^4 v_1}{\partial z^4} = 0, \tag{41}$$

and the perturbed velocity by the new scaled variables and the WKB approximation is given by Equation (31). Substituting Equations (31) and (32) into Equation (41), and taking the highest-order terms in ϵ, which is again ϵ^{-3}, we obtain

$$\frac{\partial^2 Q_0}{\partial z^2} + \frac{\omega^2}{c_s^2} Q_0 = 0, \tag{42}$$

with the boundary conditions

$$Q_0 = 0 \quad \text{at } z = \pm\frac{1}{2}. \tag{43}$$

The solution to this boundary-value problem is given by

$$Q_0(z, t_1) = \sum_{n=0}^{\infty} B_n(t_1) \cos\big((2n+1)\pi z\big), \quad \omega_n = (2n+1)\pi c_s, \ n = 0, 1, 2, \ldots, \tag{44}$$

where $B_n(t_1)$ stands for the amplitude of the longitudinal standing modes, and it is found by taking the second-highest-order terms in ϵ for Equation (41) and then using the properties of Sturm–Liouville problems as follows.

The next-largest-order terms in ϵ, of the order of ϵ^{-2}, give the equation

$$\frac{\partial^2 Q_1}{\partial z^2} + \frac{\omega^2}{c_s^2} Q_1 = \frac{\mathrm{i}}{\omega c_s^2}\left[\left(\frac{7}{2}\omega^2 + 3\omega\frac{\mathrm{d}\omega}{\mathrm{d}t_1}\right)Q_0 + 3\omega^2\frac{\partial Q_0}{\partial t_1} + c_s^2\frac{\partial^3 Q_0}{\partial t_1 \partial z^2} + \left(\frac{5}{2}c_s^2 - \tilde{\sigma}\omega^2 c_s^5\right)\frac{\partial^2 Q_0}{\partial z^2} - \tilde{\sigma}\frac{c_s^7}{\gamma}\frac{\partial^4 Q_0}{\partial z^4}\right]. \tag{45}$$

It yields from Equation (28) that Q_1 satisfies the boundary conditions

$$Q_1 = 0 \quad \text{at } z = \pm\frac{1}{2}. \tag{46}$$

Analogous to Equations (36) and (37), this boundary-value problem, Equations (45) and (46), has a solution only when the right-hand side of Equation (45) satisfies the compatibility condition. Consequently,

$$\int_{-1/2}^{1/2} \frac{\mathrm{i}}{\omega c_s^2}\left[\left(\frac{7}{2}\omega^2 + 3\omega\frac{\mathrm{d}\omega}{\mathrm{d}t_1}\right)Q_0^2 + 3\omega^2 Q_0\frac{\partial Q_0}{\partial t_1} + c_s^2 Q_0\frac{\partial^3 Q_0}{\partial t_1 \partial z^2} + \left(\frac{5}{2}c_s^2 - \tilde{\sigma}\omega^2 c_s^5\right)Q_0\frac{\partial^2 Q_0}{\partial z^2} - \tilde{\sigma}\frac{c_s^7}{\gamma}Q_0\frac{\partial^4 Q_0}{\partial z^4}\right]\mathrm{d}z = 0. \tag{47}$$

Substituting (44) into (47), we obtain the amplitude of standing wave

$$B_n(t_1) = B_n(0)\exp\left(\frac{1}{4}t_1 + \frac{\tilde{\sigma}}{5}\left(\frac{\gamma-1}{\gamma}\right)(2n+1)^2\pi^2\left[c_s^5(t_1) - 1\right]\right), \tag{48}$$

which can be re-written in the scaled variables as

$$B_n(t) = B_n(0)\exp\left(\frac{\epsilon}{4}t + \frac{\sigma}{5\epsilon}\left(\frac{\gamma-1}{\gamma}\right)(2n+1)^2\pi^2\left[c_s^5(t) - 1\right]\right), \tag{49}$$

where $c_s^5(t) = (\sqrt{T_0(t)})^5 = \exp(-5\epsilon t/2)$. Now, Equation (44), which represents a Fourier cosine series, with the boundary conditions (28) is applied to obtain the value of constants $B_n(0)$. Hence, the solution (49) is

$$B_n(t) = \alpha\exp\left(\frac{\epsilon}{4}t + \frac{\sigma}{5\epsilon}\left(\frac{\gamma-1}{\gamma}\right)(2n+1)^2\pi^2\left[c_s^5(t) - 1\right]\right), \tag{50}$$

which reveals the temporal evolution of longitudinal standing-mode amplitude due to thermal conduction in a temporally variable (cooling or heating) background plasma. Note that, in the limit $\sigma \to 0$, *i.e.* if there is no thermal conduction, Equation (50) reduces to Equation (40), which represents the amplitude variation of standing waves generated in a model of cooling plasma without non-ideal effects such as thermal conduction. Moreover, in the absence of thermal conduction, Equations (45) and (47) are converted to Equations (36) and (38), respectively; but this procedure is not straightforward because the coefficient of thermal conduction $[\kappa_\parallel]$ is a function of time and is composed of both σ and $T_0^{5/2}$ as seen in

Equation (21). Hence, we need to deal with all terms of Equations (45) and (47) to recapture Equations (36) and (38) (see the Appendix).

Expanding the sound speed by Taylor expansion and neglecting small terms of the order of ϵ^2 and higher since $\epsilon \ll 1$, Equation (50) becomes

$$B_n(t) = \alpha \exp\left(\frac{\epsilon}{4}t - \frac{\sigma}{2}\left(\frac{\gamma-1}{\gamma}\right)(2n+1)^2\pi^2\left[t - \frac{5}{4}\epsilon\, t^2\right]\right). \tag{51}$$

Subsequently, we can reveal some properties of the oscillation amplitude by examining some limitations. For instance, assume that $\epsilon = 0$, meaning there is no cooling in the model, then Equation (51) will reduce to

$$B_n(t) = \alpha \exp\left(-\frac{\sigma}{2}\left(\frac{\gamma-1}{\gamma}\right)(2n+1)^2\pi^2\, t\right), \tag{52}$$

which is identical with its counterpart in De Moortel and Hood (2003). It is clear from Equation (52) that the wave amplitude is subject to a damping, and the amount of damping depends on the value of σ.

4. Numerical Evaluations

Morton *et al.* (2010) and Erdélyi *et al.* (2011) have shown that the WKB approximation accurately estimates the solutions to the frequency and amplitude variations in time and space for waves supported by oscillating magnetic loops due to plasma cooling by radiation and/or thermal conduction, respectively. The approximate solutions obtained by the WKB theory can be motivated using numerical evaluations to demonstrate a clear view of the analytically found behaviour of MHD waves. In what follows, we display the analytical solution of the standing wave amplitude in a variable, time-dependent background plasma as derived by the WKB approximation.

The amplitude of the longitudinal (acoustic) standing waves is plotted after calculating the variables using standard coronal values. Figure 2 shows the amplitude variations due to a cooling (or heating) mechanism. This exhibits an amplification for the wave amplitude caused by the background cooling, where increasing ϵ (the ratio of the oscillation period to the cooling-time scale) increases the amplitude. This result agrees with that reached by Erdélyi *et al.* (2011), who found that the efficiency of damping is reduced by the cooling background plasma, where Figure 2 displays no damping for standing oscillations because the model is purely dominated by the cooling.

Next, in Figure 3 we demonstrate how the amplitude of standing longitudinal (acoustic) waves for a range of values of ϵ and as a function of the thermal ratio value $[\sigma]$ is changing in different temperature regions. It is found that the variation of ϵ leads to a considerable change in the damping rate of both cool and hot loops. Figure 3a illustrates the trend of the EUV (cool) loop amplitude, which is such that the oscillation amplitude decreases slowly in regions of temperature 600 000 K. The decay of the wave amplitude increases slightly with time in the hot corona, for instance in loops of temperature 3 MK and 5 MK as depicted in Figures 3b and 3c. The damping strength of hot (*e.g.* SXT/XRT) loops is found to be much stronger and shows little change for the lowest values of ϵ, *i.e.* $0.01-0.1$, whereas high enough values of ϵ, *i.e.* in the range $0.1 < \epsilon \leq 0.5$, rapidly reduce the damping rate of the wave amplitude. Moreover, it is obvious from Equation (49) that the first term in the exponential function is the same as in Equation (39), where both are dominated by the

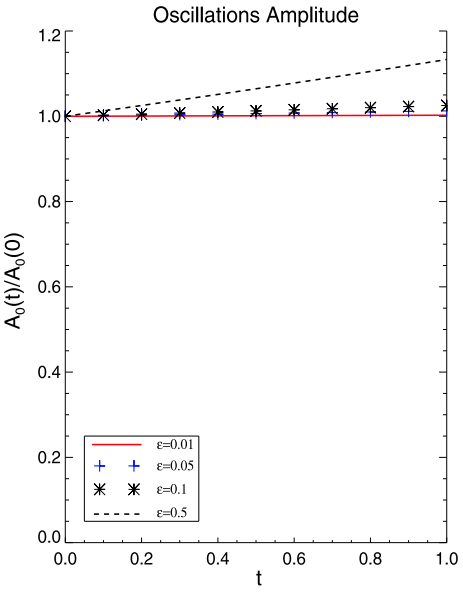

Figure 2 The amplitude of the standing wave with different values of ϵ $(0.01, 0.05, 0.1, 0.5)$ representing the ratio of the period to the cooling time.

cooling. This indicates that the emergence of cooling by a physically unspecified thermodynamic source in the system of hot coronal loops reduces the damping rate that is dominated by thermal conduction as exhibited in Figure 3.

In Figure 4 we present the effect of varying the magnitude of the thermal conduction coefficient $[\kappa]$ on the damping rate of the standing acoustic wave. Typical values for the coefficient of the thermal conductivity $\kappa = [10^{-10}, 10^{-11}, 10^{-12}]T^{5/2}$ are taken to shed light on the influence of thermal conduction on the hot corona, $T = 3$ MK, and the characteristic value of $\epsilon = 0.1$ is assumed (see Priest, 2000). It is found that the damping rate is changing fairly rapidly with altering κ by just an order of magnitude, where increasing the value of κ gives rise to a strong decline in the amplitude of the standing slow mode.

The significance of these results is to be compared to observations. We only present here a quantitative comparison with the properties of hot loop oscillations observed by SUMER (see Wang *et al.*, 2003a), where the standing slow-mode waves are detected only in the temperature region ≥ 6 MK. The oscillation periods are $7-31$ minutes. The slow standing wave has been seen to be strongly damped with characteristic decay times $5.7-36.8$ minutes, likely mainly because of thermal conduction. The typical length of coronal loops is around 230 Mm.

We found that hot-loop oscillations experience a strong damping due to thermal conduction that might be comparable with the observed damping if the value of ϵ is low enough, as shown in Figure 3c. In addition to this, Figure 4 shows that the high value of the thermal-conduction coefficient leads to rapid damping, which is likely applicable for the observed damping of standing acoustic modes as discussed by Ofman and Wang (2002) and Mendoza-Briceño *et al.* (2004).

However, the dashed line in Figure 4, which represents the standing-mode amplitude with $\kappa_0 = 10^{-10}$ at $T = 3$ MK and $\epsilon = 0.1$, is indeed stretching the theory because this result describes the wave-amplitude variation when $\sigma = 1.7$, which would not be consistent with the assumption made by the WKB approximation that determines the influence of *weak* thermal conduction ($\sigma \ll 1$), meaning the amplitude of oscillation changes slowly with time.

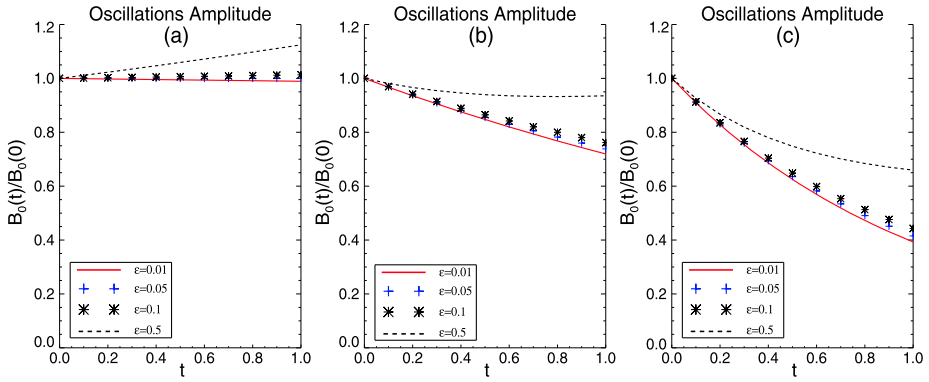

Figure 3 The amplitude of the standing wave with different values of ϵ $(0.01, 0.05, 0.1, 0.5)$ representing the ratio of the period to the cooling time and the specific value of σ, *i.e.* the thermal ratio value. (a) $\sigma = 0.0068$ ($T = 600\,000$ K), (b) $\sigma = 0.17$ ($T = 3$ MK), (c) $\sigma = 0.48$ ($T = 5$ MK).

Figure 4 The standing-wave amplitude with different values of the thermal-conduction coefficient $\kappa_0 = (10^{-10}, 10^{-11}, 10^{-12})$ and the specific value of the ratio of the period to the cooling time, $\epsilon = 0.1$, where $T = 3$ MK.

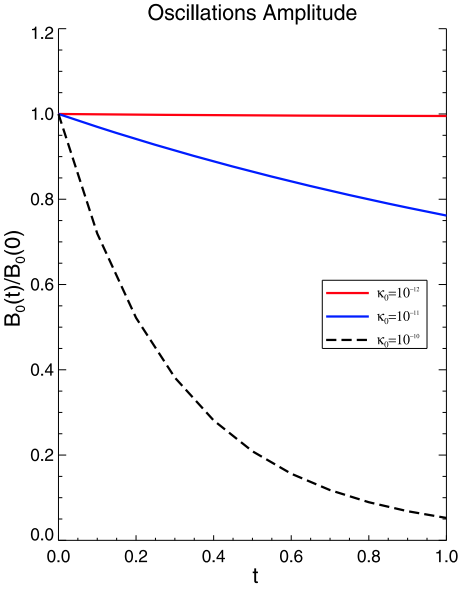

5. Discussion and Conclusion

We have investigated the influence of a cooling background on the standing magneto–acoustic waves generated in a uniformly magnetised plasma. Thermal conduction is assumed to be the dominant mechanism for the damping of hot coronal oscillations. The background temperature was allowed to change as a function of time and to decay exponentially with characteristic cooling times typical for coronal loops. The magnetic field was assumed to be constant and aligned along the z-direction, which may be a suitable model for loops with a high aspect ratio. A theoretical model of 1D geometry describing the coronal loop was applied. A time-dependant governing equation was derived by perturbing the background plasma on a time-scale greater than the period of the oscillation. Three different cases were considered: (I) absence of thermal conduction [σ] and physically unspecified cooling or

heating mechanism [$\mathcal{L}$], (II) presence of physically unknown thermodynamic source [$\mathcal{L}$] only, *i.e.* $\sigma = 0$, (III) the influence of thermal conduction [σ] combined with the physically unknown mechanism [$\mathcal{L}$].

The WKB theory was used to find the analytical solution of the governing equation in Cases II and III, where the governing equation in Case I was solved by a direct method and gave the undamped standing wave, *i.e.* the sound speed is constant. An approximate solution that describes a time-dependant amplitude of the standing acoustic mode was obtained with the aid of the properties of a Sturm–Liouville problem. The analytically derived solutions were numerically shown to illustrate the behaviour of MHD slow waves quite well.

In the second case, the individual influence of cooling background plasma on hot-loop oscillation was found to increase the amplitude of the longitudinal standing wave. The amplification rate varies according to the change in the ratio of the oscillatory period to the cooling-time scale [ϵ], where increasing ϵ increases the amplitude of the MHD wave.

In the third case, which is the focus of our interest, the temporally evolving amplitude was found to undergo a strong damping due to the influence of thermal conduction on the hot corona. In addition to this, cooling in a hot coronal-loop model reduces the damping efficiency. The ratio variation of the oscillation period to the cooling-time scale [ϵ] plays an effective role in changing the damping rate of oscillating hot coronal loops, causing a rapid decline in the decay degree of the oscillation amplitude once the value of this ratio is high enough.

These results indicate that this investigation contributes, as did previous studies (Morton and Erdélyi, 2009, 2010; Morton *et al.*, 2010; Erdélyi *et al.*, 2011), to demonstrating that the temporal evolution of coronal plasma due to the dissipative process, *i.e.* the cooling of the background plasma due to radiation/thermal conduction, has a great influence on the coronal oscillations. In the modelling of solar coronal loops, it is necessary to consider the temporal- and spatial-dependent dynamic background plasma to understand the properties of the observed MHD waves.

Acknowledgements The authors would like to thank M.S. Ruderman and R.J. Morton for useful discussions. R.E. acknowledges M. Kéray for patient encouragement. The authors are also grateful to NSF, Hungary (OTKA, Ref. No. K83133), Science and Technology Facilities Council (STFC), UK, and Ministry of Higher Education, Oman for the financial support.

Appendix

Eliminating all terms that include $\tilde{\sigma}$, Equation (45) becomes

$$\frac{\partial^2 Q_1}{\partial z^2} + \frac{\omega^2}{c_s^2} Q_1 = \frac{\mathrm{i}}{\omega c_s^2}\left[\left(\frac{7}{2}\omega^2 + 3\omega\frac{\mathrm{d}\omega}{\mathrm{d}t_1}\right)Q_0 + 3\omega^2\frac{\partial Q_0}{\partial t_1} + c_s^2\frac{\partial^3 Q_0}{\partial t_1 \partial z^2} + \frac{5}{2}c_s^2\frac{\partial^2 Q_0}{\partial z^2}\right]. \quad (53)$$

Since the second term on the right-hand side of Equation (53) can be written as

$$3\omega\frac{\mathrm{d}\omega}{\mathrm{d}t_1}Q_0 = (2+1)\omega\frac{\mathrm{d}\omega}{\mathrm{d}t_1}Q_0 = \left(-\omega^2 + \omega\frac{\mathrm{d}\omega}{\mathrm{d}t_1}\right)Q_0, \quad \text{where } \frac{\mathrm{d}\omega}{\mathrm{d}t_1} = -\frac{\omega}{2}, \quad (54)$$

and the fourth term, after using Equation (42), can have the form

$$c_s^2\frac{\partial^3 Q_0}{\partial t_1 \partial z^2} = -\omega^2\frac{\partial Q_0}{\partial t_1}, \quad (55)$$

substituting Equations (54) and (55), Equation (53) is given as

$$\frac{\partial^2 Q_1}{\partial z^2} + \frac{\omega^2}{c_s^2} Q_1 = \frac{\mathrm{i}}{\omega c_s^2}\left[\left(\frac{5}{2}\omega^2 + \omega\frac{\mathrm{d}\omega}{\mathrm{d}t_1}\right) Q_0 + 2\omega^2 \frac{\partial Q_0}{\partial t_1} + \frac{5}{2} c_s^2 \frac{\partial^2 Q_0}{\partial z^2}\right]. \tag{56}$$

Now, the first term and the last term on the right-hand side of Equation (56) can be combined to give

$$\frac{5}{2}\omega^2 Q_0 + \frac{5}{2} c_s^2 \frac{\partial^2 Q_0}{\partial z^2} = \frac{5}{2} c_s^2 \left[\frac{\omega^2}{c_s^2} Q_0 + \frac{\partial^2 Q_0}{\partial z^2}\right] = 0. \tag{57}$$

Eventually, by employing Equation (57), Equation (56) will reduce to

$$\frac{\partial^2 Q_1}{\partial z^2} + \frac{\omega^2}{c_s^2} Q_1 = \frac{\mathrm{i}}{\omega c_s^2}\left[\omega\frac{\mathrm{d}\omega}{\mathrm{d}t_1} Q_0 + 2\omega^2 \frac{\partial Q_0}{\partial t_1}\right], \tag{58}$$

which is exactly Equation (36) after taking ω as a common factor from the bracket. Similarly, we can recover Equation (38) from Equation (47).

References

Aschwanden, M.J., Terradas, J.: 2008, *Astrophys. J. Lett.* **686**, L127.
Berghmans, D., Clette, F.: 1999, *Solar Phys.* **186**, 207.
Bradshaw, S.J., Erdélyi, R.: 2008, *Astron. Astrophys.* **483**, 301.
De Moortel, I.: 2009, *Space Sci. Rev.* **149**, 65.
De Moortel, I., Hood, A.W.: 2003, *Astron. Astrophys.* **408**, 755.
De Moortel, I., Ireland, J., Walsh, R.W.: 2000, *Astron. Astrophys.* **355**, L23.
De Pontieu, B., Erdélyi, R., De Moortel, I.: 2005, *Astrophys. J. Lett.* **624**, L61.
Erdélyi, R., Taroyan, Y.: 2008, *Astron. Astrophys.* **489**, 49.
Erdélyi, R., Al-Ghafri, K.S., Morton, R.J.: 2011, *Solar Phys.* **272**, 73. ADS:2011SoPh..272...73E, doi:10.1007/s11207-011-9795-5.
Erdélyi, R., Luna-Cardozo, M., Mendoza-Briceño, C.A.: 2008, *Solar Phys.* **252**, 305. ADS:2008SoPh..252..305E, doi:10.1007/s11207-008-9274-9.
Luna-Cardozo, M., Verth, G., Erdélyi, R.: 2012, *Astrophys. J.* **748**, 110.
Mariska, J.T.: 2005, *Astrophys. J. Lett.* **620**, L67.
Mariska, J.T.: 2006, *Astrophys. J.* **639**, 484.
McEwan, M.P., De Moortel, I.: 2006, *Astron. Astrophys.* **448**, 763.
McLaughlin, J.A., Hood, A.W., De Moortel, I.: 2011, *Space Sci. Rev.* **158**, 205.
Mendoza-Briceño, C.A., Erdélyi, R., Sigalotti, L.D.G.: 2002, *Astrophys. J. Lett.* **579**, L49.
Mendoza-Briceño, C.A., Erdélyi, R., Sigalotti, L.D.G.: 2004, *Astrophys. J.* **605**, 493.
Morton, R., Erdélyi, R.: 2009, *Astrophys. J.* **707**, 750.
Morton, R., Erdélyi, R.: 2010, *Astrophys. J.* **519**, A43.
Morton, R., Hood, A.W., Erdélyi, R.: 2010, *Astron. Astrophys.* **512**, A23.
Nakariakov, V.M., Verwichte, E., Berghmans, D., Robbrecht, E.: 2000, *Astron. Astrophys.* **362**, 1151.
Nightingale, R.W., Aschwanden, M.J., Hurlburt, N.E.: 1999, *Solar Phys.* **190**, 249. ADS:1999SoPh..190..249N, doi:10.1023/A:1005211618498.
Ofman, L., Wang, T.: 2002, *Astrophys. J. Lett.* **580**, L85.
Ofman, L., Nakariakov, V.M., DeForest, C.E.: 1999, *Astrophys. J.* **514**, 441.
Ofman, L., Romoli, M., Poletto, G., Noci, C., Kohl, J.L.: 1997, *Astrophys. J. Lett.* **491**, L111.
Ofman, L., Romoli, M., Poletto, G., Noci, C., Kohl, J.L.: 2000a, *Astrophys. J.* **529**, 592.
Priest, E.R.: 2000, *Solar Magneto-Hydrodynamics*, Kluwer Academic, Dordrecht, 86.
Ruderman, M.S.: 2011, *Solar Phys.* **271**, 41. ADS:2011SoPh..271...41R, doi:10.1007/s11207-011-9772-z.
Schrijver, C.J., Title, A.M., Berger, T.E., Fletcher, L., Hurlburt, N.E., Nightingale, R.W., Shine, R.A., Tarbell, T.D., Wolfson, J., Golub, L., Bookbinder, J.A., DeLuca, E.E., McMullen, R.A., Warren, H.P., Kankelborg, C.C., Handy, B.N., De Pontieu, B.: 1999, *Solar Phys.* **187**, 261. ADS:1999SoPh..187..261S, doi:10.1023/A:1005194519642.

Sigalotti, L.D.G., Mendoza-Briceño, C.A., Luna-Cardozo, M.: 2007, *Solar Phys.* **246**, 187. ADS:2007SoPh..246..187S, doi:10.1007/s11207-007-9077-4.
Soler, R., Oliver, R., Ballester, J.L.: 2008, *Astrophys. J.* **684**, 725.
Taroyan, Y., Bradshaw, S.: 2008, *Astron. Astrophys.* **481**, 247.
Taroyan, Y., Erdélyi, R.: 2009, *Space Sci. Rev.* **149**, 229.
Taroyan, Y., Erdélyi, R., Wang, T.J., Bradshaw, S.J.: 2007, *Astrophys. J. Lett.* **659**, L173.
Verth, G., Erdélyi, R.: 2008, *Astron. Astrophys.* **486**, 1015.
Verwichte, E., Haynes, M., Arber, T.D., Brady, C.S.: 2008, *Astrophys. J.* **685**, 1286.
Wang, T.: 2011, *Space Sci. Rev.* **158**, 397.
Wang, T.J., Ofman, L., Davila, J.M.: 2009, *Astrophys. J.* **696**, 1448.
Wang, T.J., Solanki, S.K., Curdt, W., Innes, D.E., Dammasch, I.E.: 2002, *Astrophys. J. Lett.* **574**, L101.
Wang, T.J., Solanki, S.K., Curdt, W., Innes, D.E., Dammasch, I.E., Kliem, B.: 2003a, *Astron. Astrophys.* **406**, 1105.
Wang, T.J., Solanki, S.K., Innes, D.E., Curdt, W., Marsch, E.: 2003b, *Astron. Astrophys.* **402**, L17.
Wang, T.J., Solanki, S.K., Innes, D.E., Curdt, W.: 2005, *Astron. Astrophys.* **435**, 753.